Electronic and magnetic properties of Co and Ni impurities in Cu wires: First-principles investigation of local moment formation in one dimension

Matthieu Saubanère,[1] J. L. Ricardo-Chávez,[2] and G. M. Pastor[1]
[1]*Institut für Theoretische Physik, Universität Kassel, Heinrich Plett Straße 40, 34132 Kassel, Germany*
[2]*Centro Nacional de Supercómputo, IPICyT, 78216 San Luis Potosí, Mexico*
(Received 7 January 2010; revised manuscript received 9 June 2010; published 31 August 2010)

The local moment formation in one-dimensional (1D) systems is investigated in the framework of a generalized gradient approximation to density-functional theory (DFT). The electronic and magnetic properties of Co and Ni impurities in finite Cu wires are determined as a function of experimentally relevant parameters such as wire length, impurity-host distance, impurity position within the wire, and total spin polarization S_z. Results are given for the interatomic equilibrium distances, relative stability of different total spin configurations, local magnetic moments in both Wigner-Seitz and Bader cells, electronic density of states at the impurity, and induced magnetic moments in the 1D metal including their coupling with the impurity. The calculations show that the optimal total spin polarization is one above the minimal value. In fact, for chains having an even number of Cu atoms, the ground-state total spin is $S_z=1$ for Ni-doped wires and $S_z=3/2$ for Co-doped wires. Both Co and Ni impurities preserve their magnetic degree of freedom and develop large local magnetic moments in all low-lying spin configurations ($S_z \leq 5/2$). These almost completely saturated impurity moments are largely dominated by the *d*-electron contributions. In the ground-state the magnetic coupling between the impurity and the induced moments at the host atoms is ferromagneticlike. Thus, the local exchange energy dominates over hybridization and spin-fluctuation effects, at least in the framework of the present approximation to DFT. The local density of electronic states (LDOS) at the impurity is found to have essentially *d* character in the whole valence-band range. Large exchange splittings consistent with saturated *d* moments are observed, which imply a full minority-spin polarization of the LDOS at the Fermi energy ε_F. A remarkable correlation is revealed between the rotational symmetry and the degree of delocalization of the impurity states close to ε_F. Trends as a function of the local atomic environment are discussed.

DOI: 10.1103/PhysRevB.82.054436 PACS number(s): 75.75.−c, 75.20.Hr, 73.22.−f

I. INTRODUCTION

Low-dimensional nanostructures constitute a vast research area with multiple subfields and a truly multidisciplinary character. Strong electron-correlation effects and in particular magnetism are one of its most interesting and challenging topics. Over the past years a remarkably intense activity has developed in this context, which ranges from experimental and theoretical basic investigations all over to materials-science studies geared to technological applications.[1,2] Recent progress in atomic manipulation by scanning tunneling microscopy (STM) and diffusion-controlled aggregation has opened the way to the preparation of a variety of nanostructures at surfaces including small particles, one-dimensional (1D) wires and two-dimensional islands of various sizes, structures and chemical compositions.[3–15] The experimental investigations performed on these atom-by-atom engineered structures have revealed a number of amazing effects such as the enhancement of orbital magnetism and magnetic anisotropy,[3,4] long-range atomic ordering of adatoms,[5–7] magnetization reversal and spin reorientation transitions in deposited clusters,[8,9] as well as noncollinear spin arrangements, quantum confinement and self-alignment of magnetic moments in nanowires.[10–15] Low-dimensional magnetic nanostructures define therefore a remarkable scenario where a number of current fundamental experimental and theoretical interests merge.

In solids, transition-metal (TM) and rare-earth compounds show fascinating properties, such as Kondo, intermediate-valence, or heavy-fermion behaviors, which are intrinsically related to the localized character of the *d* or *f* electrons and to their interactions with the conduction-band states.[16] The unconventional properties of such strongly correlated systems reflect the competition between the tendency of electrons to delocalize, in order to form chemical bonds and energy bands, and the resulting local charge fluctuations, which increase the Coulomb-repulsion energy and which favor the formation of localized states. A typical manifestation of this interplay is the presence of small energy scales in the excitation spectrum that lead to striking low-temperature properties.[17,18] Clearly, the reduction in dimensionality found in nanostructures (e.g., clusters, wires or surfaces) can drastically modify and eventually suppress these phenomena. The environment dependent changes in the impurity-host hybridizations, in the electronic density of conduction states near the Fermi level, or in the interatomic distances and lattice structure are expected to alter the conditions for the stability of local magnetic moments, the type of magnetic coupling between the impurity and the metal host, as well as the relevant spin-fluctuation energy scales. In past years the consequences of confinement and of the discreteness of the energy spectrum have been investigated theoretically by considering the single-impurity Anderson model[19] in quantum boxes[20] and small clusters.[21,22] More recently, a number of experimental and theoretical studies have been devoted to the magnetic behavior of Co impurities in Cu chains,[12,13] islands,[23] and surfaces.[24,25] These have renewed the interest in the problem of local moment formation and quantum spin

fluctuations in 1D nanostructures. Besides exploring the usual dependence of the spin-polarized electronic density and of the single-particle electronic spectrum on size and dimensionality, one would like to understand the consequences of changing the local atomic environment on the degree of localization of the impurity states. This is expected to profoundly affect the subtle many-body phenomena behind the spin-excitation spectrum even at a qualitative level, for example, concerning the behavior of the ground-state and of the low-lying excitations. In this context, DFT is undoubtedly the most successful first-principles approach for elucidating the ground-state properties of magnetic materials. Yet, the functionals at our disposal are known to be fallible. For example, the ordering of the energy levels as a function of the total spin may be distorted by unavoidable mean-field and symmetry-breaking approximations. Nevertheless, it is very important to investigate the development of local magnetic moments in nanostructures and the magnetic coupling between the impurity and the metal host in the framework of DFT. Besides their specific theoretical interest, such studies provide the basis for any further developments in the direction of many-body spin fluctuations and Kondo-type screening.

The purpose of this paper is to survey the electronic and magnetic properties of magnetic impurities in simple-metal nanowires, taking Co- and Ni-doped monoatomic Cu chains as particularly relevant examples. To this aim we have performed a series of first-principles calculations in the framework of DFT by considering finite monoatomic wires having $N \leq 13$ atoms. The main details of the computational procedure are given in Sec. II while the actual results are presented in Sec. III. Here we discuss the relative stability of the relevant lowest-energy spin-configurations, the corresponding magnetic moment at the impurity atom and their coupling with the moments induced at the simple-metal host, the environment dependence of the local electronic structure, as well as the dependence of the magnetic moments and bond-length relaxation on the position of the impurity within the wire. Finally, in Sec. IV the main trends are summarized together with a brief outlook on interesting future extensions.

II. COMPUTATIONAL DETAILS

The calculations reported in the present work have been performed in the framework of Hohenberg-Kohn-Sham's (KS) density-functional theory,[26] as implemented in the Vienna *ab initio* simulation package (VASP).[27] The exchange and correlation energy-functional is treated by using Perdew and Wang's spin-polarized generalized-gradient approximation (GGA).[28] In the program VASP the spin-polarized Kohn-Sham equations are solved in an augmented plane-wave basis set, taking into account the interaction between valence electrons and ionic cores by using the projector-augmented wave (PAW) method.[29] This is an efficient frozen-core all-electron approach, which takes into account the proper nodes of the valence KS orbitals in the core region and the resulting effects on the electronic structure and magnetic properties. For the present calculations on $3d$ TM compounds, the default PAW potentials were generated by keeping the $4s$, $4p$, and $3d$ orbitals as valence electrons.

The electronic and magnetic properties of magnetic impurities in 1D wires have been studied by considering a series of finite monoatomic Cu chains, in which a Ni or Co impurity occupies various substitutional positions. Different kinds of magnetic couplings between the impurity and the 1D metal host are investigated by taking into account all relevant low-lying spin solutions of the KS equations. These correspond to the most stable values of the total spin polarization $S_z=(N_\uparrow - N_\downarrow)/2$, where $N_\uparrow(N_\downarrow)$ refers to the number of up (down) electrons. Depending on the value of S_z one observes parallel or antiparallel arrangements of the local magnetic moments of the impurity and of the surrounding noble-metal atoms. In practice, the calculations are performed for $S_z=0$, 1, and 2 in Cu_mNiCu_n, and for $S_z=1/2$, 3/2, and 5/2 in Cu_mCoCu_n. For simplicity we focus on even numbers $m+n$ of Cu atoms in the wire ($m+n \leq 12$). For each chain length and spin configuration, we consider a rectangular periodic cell whose dimensions are large enough so that the interaction between the images of the wire can be neglected. The typical distance between images in the present calculations is larger than 10 Å. The atomic positions are relaxed self-consistently keeping the 1D constraint, until the Hellmann-Feynman forces $\vec{F}_i$ on each atom i almost vanish. In practice we assume that this condition is met when $|\vec{F}_i| \leq 0.01$ eV/Å for all i. The electronic calculations are performed at a standard level of precision. In particular the default value of the energy cutoff of the plane waves is $E=274$ eV.[30] It should be also noted that the high symmetry of the chains introduces some difficulties in the convergence of the KS orbitals and eigenenergies near the Fermi level. For this reason special attention has been paid to the choice of the parameter σ by which the discrete energy levels are smeared.[31] Several calculations are in fact performed by reducing σ systematically until the residual contribution of the entropy to the total energies is less 10^{-2} meV per atom. This is consistent with the convergence criterion for the electronic part.[30]

The wire properties are determined as a function of length by considering both symmetric and nonsymmetric impurity positions. In each case, we determine the relative stability of the low-lying spin states by computing the magnetic excitation energy $\Delta E_m(S_z)=E(S_z)-E(S_z^0)$ with respect to the ground-state spin S_z^0. Other relevant quantities for the analysis of the electronic properties are the local atomic charges ν_i and magnetic moments μ_i. These are calculated by considering both the Wigner-Seitz (WS) sphere and the Bader cell as integration volumes for each atom i.[32] The WS sphere, centered at the atomic position, takes into account mainly the localized part of the charge and magnetic moment. In order to be able to compare the results for different wire length and impurity positions, we consider the same WS radius in all the calculations: $R_{WS}=1.312$, 1.286, and 1.302 Å for Cu, Ni, and Co, respectively. The Bader basin has been determined following the atoms in molecules approach[32] by using the numerical algorithm developed by Henkelman.[33] Let us recall that a point $\vec{r} \in \mathbb{R}^3$ belongs to the Bader basin or cell of atom i, if one reaches the atomic position $\vec{R}_i$ by starting from $\vec{r}$ and by following the gradient of the self-consistent electronic density $n(\vec{r})$. Notice that the union of the Bader cells

of all atoms cover $\mathbb{R}^3$. In contrast to the WS cell, the Bader volume associated to an atom depends on its position in the system. It bares little or no relation to the volume per atom, specially at low-coordinated sites. Bader's method takes properly into account spill-off effects, the interstitial contributions of the charge density, as well as the environment-dependent local symmetry. However, the results cannot be easily projected on spherical harmonics. It is therefore difficult to discern between s, p, and d contributions to the local moments. The average within Bader cells gives only information on the participation of each atom i as a whole. The same holds for other electronic properties that are meaningfully projected according to the rotational symmetry of the different local orbitals α. A particularly relevant property is the orbital- and spin-projected local density of states (LDOS) $\rho_{i\alpha\sigma}$. Within the WS sphere this is defined as

$$\rho_{i\alpha\sigma}(\varepsilon) = \sum_k |\langle \varphi_{i\alpha} | \Psi_{k\sigma} \rangle_{\mathrm{WS}}|^2 \delta(\varepsilon - \varepsilon_{k\sigma}), \qquad (1)$$

where $\Psi_{k\sigma}$ and $\varepsilon_{k\sigma}$ stand for the KS orbitals and eigenenergies, $\varphi_{i\alpha}(\vec{r})$ refers to the local orbital α at atom i (α=s, p, and d), and the overlap $\langle \varphi_{i\alpha} | \Psi_{k\sigma} \rangle_{\mathrm{WS}}$ is computed by considering the WS cell as integration volume. Local properties computed in the WS or PAW spheres and in the Bader cells yield thus useful complementary informations.

III. RESULTS

This section presents the results of a series of first-principles calculations on Cu wires doped with a single Ni or Co impurity. After discussing the behavior of symmetric chains we focus on the magnetization profiles, the magnetic order and the local electronic structure. Finally, we investigate the dependence of the electronic and magnetic properties on bond-length relaxation, as well as the role of the impurity position within the wire.

A. Relaxed Cu_mNiCu_m and Cu_mCoCu_m chains

We consider a magnetic impurity in a symmetric position at the center of the chain and explore the properties of the wire as a function of the number m of Cu atoms at each side of the impurity. In Figs. 1 and 2 results are given for representative electronic, magnetic, and structural properties of Cu_mNiCu_m and Cu_mCoCu_m chains. This includes the relative stability or spin-excitation energy $\Delta E_m = E(S_z) - E(S_z^0)$ between the lowest state having total spin polarization S_z and the ground state, the corresponding local magnetic moments μ_α at the impurity (α=Ni or Co), and the optimized interatomic distances between the impurity and the Cu nearest neighbors (NN). First of all one observes that for all considered chain lengths the most stable total spin is $S_z^0 = 1$ in Cu_mNiCu_m and $S_z^0 = 3/2$ in Cu_mCoCu_m. This corresponds to the polarization of one electron above the minimal-spin state having $S_z = 0$ or 1/2, the latter being in general the second-best spin configuration. Only for Co-doped wires and $m \geq 4$ we find that the $S_z = 5/2$ state has nearly the same energy or is slightly more stable than the $S_z = 1/2$ state. In general the chain length m does not affect neither the relative ordering of

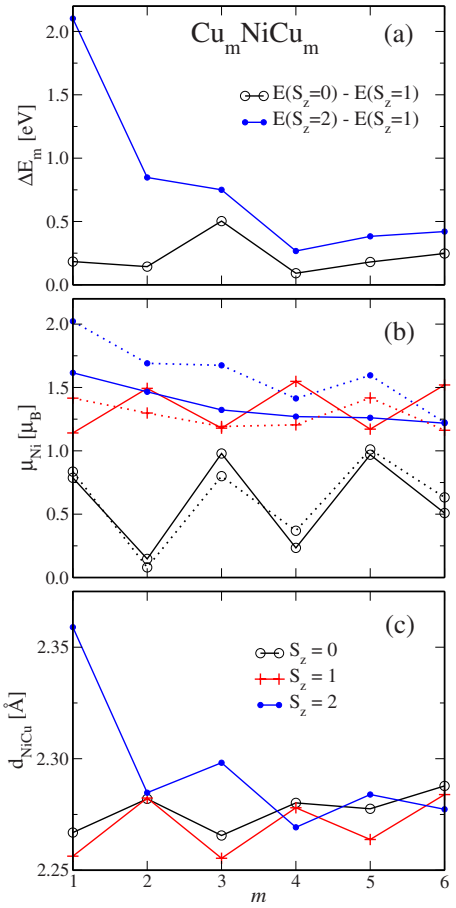

FIG. 1. (Color online) Electronic, magnetic, and structural properties of symmetric Cu_mNiCu_m wires as a function of m: (a) magnetic excitation energy $\Delta E_m = E(S_z) - E(S_z^0)$ with respect to the ground state having $S_z^0 = 1$. (b) Local magnetic moment at the Ni atom within the WS sphere (full lines) and within the Bader atomic cell (dotted lines). (c) Equilibrium interatomic distance d_{NiCu} between the Ni impurity and its Cu nearest neighbors. Circles refer to $S_z = 0$, crosses to $S_z = 1$, and dots to $S_z = 2$. The lines connecting the points are a guide to the eyes.

the different S_z states nor the ground-state configuration. In the case of Ni there are interesting even-odd oscillations of ΔE_m, which can be correlated with the oscillations of the NiCu distance d_{NiCu}. The weak dependence of $E(0) - E(1)$ in Ni-doped chains and of $E(1/2) - E(3/2)$ in Co-doped chains as a function of m suggests that the energy associated to a change in S_z is the result of a localized change in the magnetic coupling between the impurity and the surrounding s electrons. In contrast, the excitation energies to higher-spin states, $\Delta E_m = E(2) - E(1)$ for Ni and $\Delta E_m = E(5/2) - E(3/2)$ for Co, are significantly enhanced particularly for small m. The rapid decrease in these high-spin excitation energies is mainly a consequence of the length dependence of the gap in the single-particle spectrum of the chains. It can be shown that the spin excitation from $S_z = 1$ (3/2) to $S_z = 2$ (5/2) for Ni-doped (Co-doped) chains is essentially the result of the promotion of the highest occupied minority-spin electron to the first unoccupied majority-spin level within the Cu conduction band. Consequently, as m increases the gap is reduced roughly as $\Delta E_m \propto 1/m$. Moreover, the quantitative val-

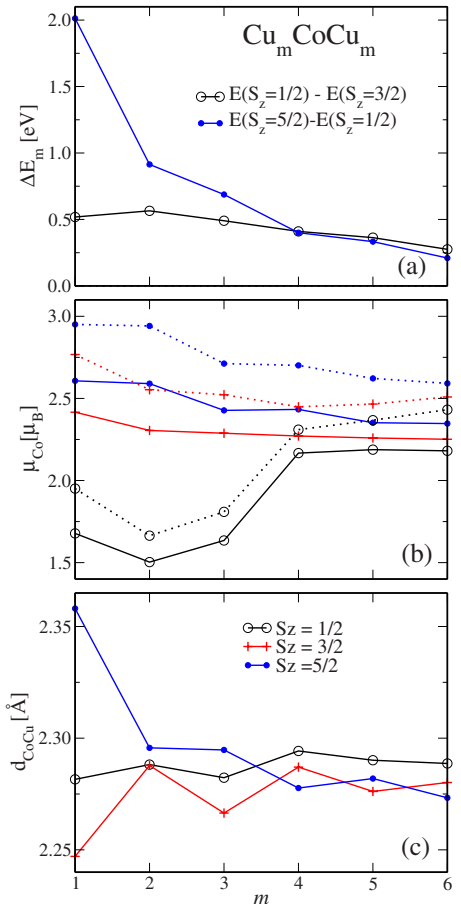

FIG. 2. (Color online) Electronic, magnetic, and structural properties of symmetric Cu_mCoCu_m wires as a function of m: (a) magnetic excitation energy $\Delta E_m = E(S_z) - E(S_z^0)$ with respect to the ground state having $S_z^0 = 3/2$. (b) Local magnetic moment at the Co atom within the WS sphere (full lines) and within the Bader atomic cell (dotted lines). (c) Equilibrium interatomic distance d_{CoCu} between the Co impurity and its Cu nearest neighbors. Circles refer to $S_z = 1/2$, crosses to $S_z = 3/2$, and dots to $S_z = 5/2$. The lines connecting the points are a guide to the eyes.

ues of ΔE_m are very similar in the case of Ni [Fig. 1(a)] and Co impurity [Fig. 2(a)]. This is consistent with the fact that the corresponding single-particle gaps in Cu_mNiCu_m, Cu_mCoCu_m, and Cu_{2m+1} are similar. For instance, for $m=1$ and $(m=2)$ one obtains $\Delta E_m = 2.1$ (0.65), 2.0 (0.9), and 2.1 (1.2) eV for Cu_mNiCu_m, Cu_mCoCu_m, and Cu_{2m+1}, respectively.

The local magnetic moments at the impurity have been determined by considering two different integration volumes as described in Sec. II The first one is the WS sphere, which takes into accounts the localized part of the magnetic moment, and the second one is the Bader atomic cell,[32] which respects the symmetry of the lattice and includes both interstitial and spill-off contributions. In the ground state $(S_z = 1)$ the value of the local moment μ_{Ni}^{WS} in the WS sphere remains always above $1\mu_B$ showing significant even-odd oscillations. In fact, μ_{Ni}^{WS} is larger for even m than for odd m [see crosses with full line in Fig. 1(b)]. This corresponds to a maximal polarization of the Ni d shell, whose average occupation ν_d within the WS sphere oscillates as a function of m. For instance, $\nu_d = 7.95$ $(\nu = 8.56)$ and $\mu_d = 1.45\mu_B$ for $m=4$ while $\nu_d = 8.30$ $(\nu = 8.91)$ and $\mu_d = 1.11\mu_B$ for $m=5$. Notice that the total number of electrons ν in the WS sphere follows the same trend. In contrast, the impurity moment in the Bader cell μ_{Ni}^{B} is essentially independent of m, showing no sign of even-odd alternations. For odd m μ_{Ni}^{B} is very close to μ_{Ni}^{WS} while for even m the latter are significantly enhanced by about $0.2-0.4\mu_B$. This behavior can be understood by analyzing the shape of the delocalized s-like orbitals close to the Fermi energy and the charge transfer between s and d orbitals. The relative large values of μ_{Ni}^{WS} in Cu_mNiCu_m with $m = 2$, 4, and 6 are the result of a d to s charge transfer. The resulting increase in the number of d holes enhances the magnetic moment in the WS sphere, which has an essentially localized d character. The transferred d electrons for even m (typically $\Delta\nu_d \simeq 0.4$) are minority electrons that occupy delocalized states in the interstitial and spill-off regions associated to the impurity atom. In this case the d to s charge transfer occurs mainly locally at the impurity site (within the Bader cell). Therefore, the extra minority s electrons yield a negative contribution to μ_{Ni}^{B}, which compensates the enhancement of the localized part, so that essentially no even-odd alternations in μ_{Ni}^{B} are observed.

The previous oscillatory behavior of the localized d impurity moment is not present in the case of Co-doped wires. As shown in Fig. 2(b) the Co moment in the WS cell shows a very weak dependence on m. Quantitatively, $\mu_{Co}^{WS} \simeq 2.3\mu_B$ in the lowest energy $S_z = 3/2$ state, which corresponds to an almost complete polarization of the d shell. The Bader moment μ_{Co}^{B} is always about $0.2-0.3\mu_B$ larger than μ_{Co}^{WS} for all considered $S_z \leq 5/2$. This implies that the more delocalized electrons beyond the WS radius of the Co atom always align parallel to the impurity moment. Moreover, the relatively strong spin polarization of the Co atom is not much affected by any changes in the hybridization or in the shape of the delocalized electron density. Increasing the total spin polarization to $S_z = 5/2$ yields, as expected, an increase in both μ_{Co}^{WS} and μ_{Co}^{B}. However, the enhancement of the impurity moments $(\Delta\mu \simeq 0.1-0.2\mu_B)$ amounts only to a small part of the increase in the total spin polarization.

Concerning the high-spin (HS) states $(S_z = 2$ or $5/2)$ one observes that the wire-length dependence of the Ni or Co impurity moment is much weaker than in the ground state. Moreover, the Bader moments are in this case always larger that the WS moments. This indicates that the details of the electronic structure and hybridizations are not so important for large S_z since the delocalize electrons are also strongly polarized. Notice that in the low-spin (LS) solutions $(S_z = 0$ or $1/2)$ the length dependence of the local moments is different from the one found in the other spin states. For Ni one observes strong even-odd oscillations of μ_{Ni} as a function of m. For odd m a localized impurity moment of about $1\mu_B$ is obtained in both the WS and Bader cells while for even m the Ni moment is nearly quenched. The origin of these oscillations can be traced back to the length dependence of the KS spectrum. The crucial point is the relative stability between xy and x^2-y^2 states, which are quite localized at the impurity atom, and the xz, yz, or $3z^2-r^2$ states, which are delocalized throughout the whole wire. For even m a

minority-spin localized Ni d state with xy symmetry is occupied and therefore μ_{Ni} is nearly quenched. In contrast, for odd m, this localized minority-spin orbital lies above ε_F. Consequently, the lack of the corresponding minority-spin density enhances μ_{Ni} to values close to $1\mu_B$.

A reduction in the impurity magnetic moment is also observed in short $\mathrm{Cu}_m\mathrm{CoCu}_m$ chains ($m \leq 3$) where $\mu_{\mathrm{Co}} \simeq 1.5-1.7\mu_B$. Nevertheless, as m increases ($m \geq 4$) the Co impurity reaches its saturated value more rapidly than in the case of Ni. This behavior can be interpreted by noting that for small m it is energetically unfavorable to polarize the amount of delocalized electrons that would be necessary to compensate a strong Co moment in the LS state. Therefore, selfconsistency is achieved by reducing μ_{Co}. For larger chains, however, it is easier to polarize the delocalized electrons since the energy gaps in the conduction band are smaller (higher DOS). Thus, the impurity can preserve its full magnetic moment, giving rise to an antiferromagnetic (AF) kind of coupling between the impurity and the conduction states.

In part (c) of Figs. 1 and 2 the equilibrium NN distances d_{NiCu} and d_{CoCu} between the impurity and the Cu host are given as a function of wire length. For small m one finds important even-odd oscillations, which eventually tend to disappear as m increases. Putting these oscillations aside, one observes that d_{NiCu} and d_{CoCu} decrease with decreasing m, as long as the spin polarization is not too large (i.e., for $S_z \leq 3/2$). Here the hybridization and bonding effects are most important. This reflects a tendency to stronger sd bonding that is well-known from finite-cluster studies.[21] On the other side, in the HS states, the opposite trend is observed, namely, larger impurity-host distances for the shortest chains. This corresponds to a weaker bond strength in magnetic configurations where the spins of the delocalized electrons align parallel to the impurity moment. A similar spin-dependent trend in the impurity-host NN distance has been observed in small Cu clusters doped with magnetic impurities.[21]

B. Magnetization profiles

The local magnetic moments μ_i at different atoms i have been determined in order to quantify the magnetic coupling between the impurity and the Cu atoms for the most stable values of the total spin polarization S_z. In this way the nature of the spin-density distribution induced by the impurity in the simple-metal 1D host can be inferred. In Figs. 3 and 4 results are given for μ_i inside the Bader cells of representative $\mathrm{Cu}_m\mathrm{NiCu}_m$ and $\mathrm{Cu}_m\mathrm{CoCu}_m$ wires having $m=4$ and 5. In the ground-state configuration ($S_z=1$) Ni-doped wires show a strong localized moment at the impurity $\mu_{\mathrm{Ni}}^{\mathrm{B}}=(1.2-1.4)\ \mu_B$, which is actually larger than the value expected for Ni in a $3d^9$ electronic configuration (see Fig. 3). For $m=4$ this is the result of an even larger d moment localized in the WS sphere, which is partly compensated by the more delocalized spin density beyond the WS radius. In contrast, for $m=5$ the impurity moment is essentially given by the spin density localized within the WS sphere. The charge distribution within the wire provides further insight on the quantitative values of local magnetic moments. In Table I the total electronic charge and magnetic moment integrated within the Bader cell of the impurity are reported. A tendency to charge transfer from the Ni impurity to the Cu host is observed, in particular for odd m (0.1–0.2 electrons). The reduction in the number of d electrons is in general stronger. Consequently, the large number of d holes allows the development of spin polarizations which appreciably surpass typical Ni values.

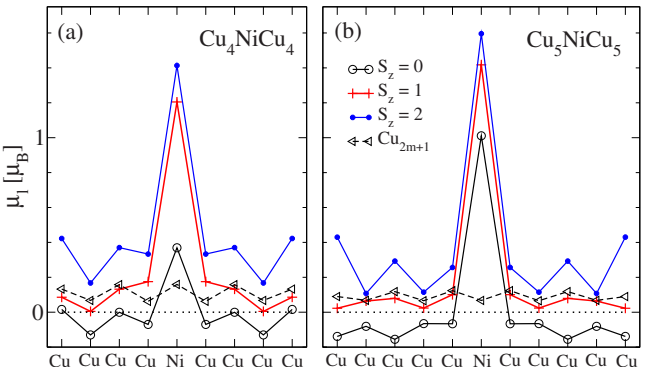

FIG. 3. (Color online) Local magnetic moment μ_i in the Bader atomic cells of (a) $\mathrm{Cu}_4\mathrm{NiCu}_4$ and (b) $\mathrm{Cu}_5\mathrm{NiCu}_5$. Circles refer to $S_z=0$, crosses to $S_z=1$, and dots to $S_z=2$. Results for the ground state of the corresponding pure Cu_{2m+1} wires are also shown ($S_z=1/2$, triangles). The lines connecting the points are a guide to the eyes.

It should be also noted that the Ni moment is well below the $2\mu_B$ total spin polarization of the wire ($S_z=1$). This implies that the Cu atoms are also polarized, showing a parallel ferromagneticlike coupling with the Ni moment. In fact the Cu μ_i are comparable to the moments found in pure Cu chains with an odd number of atoms and $S_z=1/2$. See the dashed lines with triangles in Fig. 3. Although the μ_i of the Cu atoms are very small, they amount altogether to about $0.75\mu_B$. If one increases the total spin polarization to $S_z=2$, the Ni moment is moderately increased by an amount comparable to the enhancement of μ_i in the Cu cells. Moreover, the magnetization profile for $S_z=2$ is ferromagneticlike, quantitatively similar to the ground-state one, but with larger

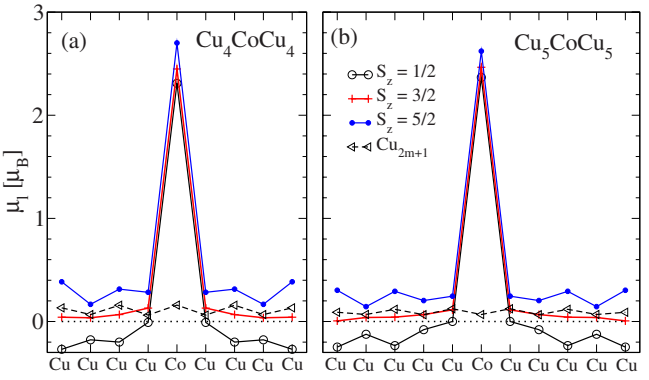

FIG. 4. (Color online) Local magnetic moment μ_i in the Bader atomic cells of (a) $\mathrm{Cu}_4\mathrm{CoCu}_4$ and (b) $\mathrm{Cu}_5\mathrm{CoCu}_5$. Circles refer to $S_z=1/2$, crosses to $S_z=3/2$, and dots to $S_z=5/2$. Results for the ground state of the corresponding pure Cu_{2m+1} wires are also shown ($S_z=1/2$, triangles). The lines connecting the points are a guide to the eyes.

TABLE I. Local electronic charge ν and magnetic moment μ in the Bader (Wigner-Seitz) cell of the magnetic impurity in Cu_mNiCu_m and Cu_mCoCu_m wires.

	Cu_mNiCu_m		Cu_mCoCu_m	
m	ν	μ	ν	μ
1	9.82 (9.01)	1.42 (1.14)	8.58 (7.73)	2.77 (2.41)
2	9.98 (8.66)	1.30 (1.49)	8.79 (7.79)	2.55 (2.30)
3	9.80 (8.91)	1.19 (1.18)	8.63 (7.77)	2.52 (2.29)
4	9.97 (8.56)	1.20 (1.55)	8.82 (7.78)	2.45 (2.27)
5	9.88 (8.91)	1.42 (1.17)	8.66 (7.78)	2.47 (2.26)
6	9.80 (8.57)	1.31 (1.52)	8.71 (7.79)	2.51 (2.25)

Cu polarizations (see Fig. 3). This confirms the idea that the Ni moment is essentially saturated already in the $S_z=1$ state, and that the spin excitation from $S_z=1$ to $S_z=2$ corresponds to an electron-hole excitation in the delocalized band of the Cu host.

In the case of Cu_mCoCu_m wires the trends are similar to those found in Cu_mNiCu_m. The main difference is that the Co impurity develops a more important localized magnetic moments which gives the largest part of the spin polarization of the chain. The Cu atoms have therefore smaller magnetic moments in both the $S_z=3/2$ and $S_z=5/2$ states. The trend to very large Co moments, well beyond $2\mu_B$, can be understood by looking at the charge distribution. As shown in Table I, there is a significant charge transfer (0.2–0.4 electrons) from the Co impurity to the Cu atoms, which is actually even stronger if one considers the d electron charge. The larger number of d holes and the fact that these are fully polarized explains the significant enhancement of the local Co moments.

A qualitatively different behavior is found in the LS solutions. In fact, the most remarkable feature found for $S_z=0$ in Cu_mNiCu_m and for $S_z=1/2$ in Cu_mCoCu_m is the change from FM to AF magnetic coupling between the impurity and the host atoms. This is consistent with the tendency to develop a strong local magnetic moment at the impurity while keeping the constraint of minimal total moment. One may further notice that the Ni impurity shows a more subtle dependence on the parity of m than Co. For $S_z=0$ and even m the Ni moment is significantly quenched as a result of hybridizations (e.g., $\mu_{Ni}=0.37\mu_B$ in Cu_4NiCu_4) while for odd m a strong local Ni moment is found (e.g., $\mu_{Ni}=1.01\mu_B$ in Cu_5NiCu_5, see Fig. 3). As already discussed, these finite-size even-odd alternations are a consequence of the symmetry of the KS orbitals at Fermi energy, on which the Ni moments depend strongly. In contrast, the Co moments are not only larger but also more robust, showing in general a much weaker dependence on wire length, even in the LS state ($m \geq 4$).

It should be finally noted that both Ni and Co impurities induce magnetic moment on the Cu atoms, which oscillate as a function of the distance to the impurity. The size of the Cu moments is actually quite larger than in the case of pure Cu_{2m+1} chains having $S_z=1/2$. It is also interesting to note that the phase of these oscillations (i.e., whether a Cu atom has larger or smaller μ_i than its neighbors) depends on S_z and on the distance to the wire edge. However, it seems to be independent of the particular $3d$ magnetic impurity (Ni or Co) and on the wire length m provided that the wire edge is taken as reference (see Figs. 3 and 4).

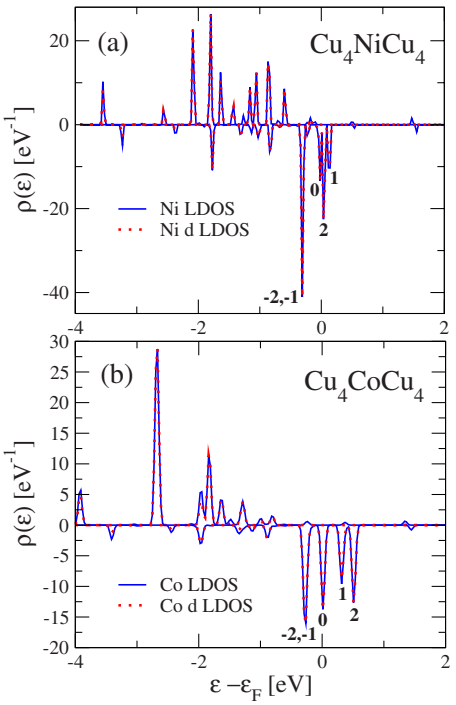

FIG. 5. (Color online) Spin-polarized LDOS at the impurity atom in (a) Cu_4NiCu_4 and (b) Cu_4CoCu_4 wires as a function of the energy ε relative to the Fermi energy ε_F. Results are given for the total LDOS (full curves) and for the d-electron LDOS (dotted curves). Positive (negative) values correspond to majority (minority) spin. The numbers label the minority-spin states k which are illustrated in Table II.

C. Local electronic structure

Further details on the electronic structure of the wires and on the microscopic origin of the impurity magnetic degree of freedom can be obtained by analyzing the LDOS. In Figs. 5 and 6 the total and d-electron LDOS at the impurity WS sphere are shown for Cu_mNiCu_m and Cu_mCoCu_m wires in the ground-state magnetic configuration ($m=4$ and 5). The dominant role played by the d-electron states is clearly illustrated by the fact that the total and d-electron LDOS are nearly indistinguishable. Both Ni and Co show important exchange splittings and a completely filled majority d band. This implies that the impurity has an essentially saturated d moment. As already discussed, the electronic configuration is qualitatively not very far from d^9s^1 for Ni and d^8s^1 for Co. However, there are clear signs of charge transfer from the impurity to the Cu atoms, which leads to an increase in the number of d holes and of the impurity moment beyond $1\mu_B$ for Ni and $2\mu_B$ for Co (see Table I). Furthermore, the nearly 100% spin polarization of the impurity states at the Fermi energy (only minority d states) should be detectable by means of spin-polarized scanning tunnel spectroscopy

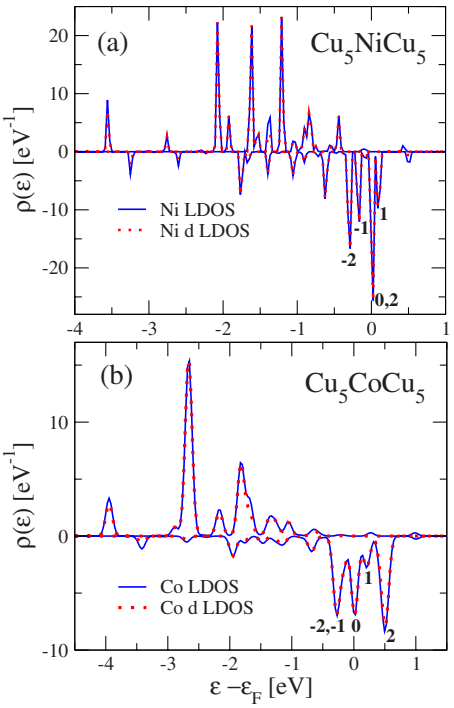

FIG. 6. (Color online) Spin-polarized LDOS at the impurity atom in (a) Cu_5NiCu_5 and (b) Cu_5CoCu_5 wires as a function of the energy ε relative to the Fermi energy ε_F. Results are given for the total LDOS (full curves) and for the d-electron LDOS (dotted curves). Positive (negative) values correspond to majority (minority) spin. The numbers label the minority-spin states k which are illustrated in Table II.

(SP-STS) particularly by taking advantage of the spatial resolution and the contrast to the weakly polarized Cu atoms (see also Figs. 3 and 4).

The differences in the majority and minority spectra of the impurity are quite remarkable. While the minority impurity d band is extremely narrow ($W_{d\downarrow} \simeq 0.5$ eV in Cu_5NiCu_5 and $W_{d\downarrow} \simeq 0.9$ eV in Cu_5CoCu_5) the majority band is significantly broader ($W_{d\uparrow} \simeq 3.0$ eV in Cu_5NiCu_5 and $W_{d\uparrow} \simeq 3.4$ eV in Cu_5CoCu_5). Actually, the latter should still be regarded as narrow, due to the reduced dimensionality and coordination number. These differences reflect a different degree of hybridization and participation in the bonding of spin up and spin down impurity orbitals. The non-negligible width of the majority d band suggests that these orbitals are indeed involved in binding and charge fluctuations, at least according to DFT. Comparing Ni- and Co-doped chains one observes a somewhat narrower d band in the former case, particularly for the minority states. It would be interesting to contrast these trends with SP-STS experiments.

A further remarkable finding is the 100% minority-spin polarization of the impurity at the Fermi energy. The spin-density distributions of the corresponding minority states close to ε_F of the Cu_5CoCu_5 chain are given in Table II. These results are also representative of Ni-doped chains as well as of other chain lengths. First of all, one observes that the impurity d orbital always play a central role close to ε_F. Therefore, the ordering and occupation of these states are most relevant for the magnetic behavior. An analysis of the

TABLE II. (Color online) Illustration of the charge-density distribution in the minority-spin orbitals $\Psi_{k\downarrow}$ close to the Fermi energy ε_F of Cu_5CoCu_5. The labeling k of the states is given in Fig. 6(b). The correlation between rotational symmetry (given in the right column) and the degree of delocalization also applies to Ni-doped chains as well as to other chain lengths (see also Figs. 5 and 6).

k	Orbital	Symmetry
−2		xy
−1		xz, yz
0		xz, yz
1		$3z^2-r^2$
2		x^2-y^2

rotational symmetry of the KS orbitals and of the corresponding degree of delocalization within the chain reveals a remarkable correlation. While the xz, yz, and z^2-3r^2 states are delocalized throughout the chain, the xy and x^2-y^2 are strongly localized at the impurity, involving only weak contributions from the d orbitals of the NN Cu atoms (see Table II). This can be explained by noting that symmetry precludes any hybridization between xy or x^2-y^2 impurity orbitals and the Cu s or p orbitals. As shown in Table II the differences in the degree of delocalization among the various states are quantitatively important. Similar strong effects should be observable in STM experiments for different bias voltages. It should be noted that the relative stability of the various states near ε_F (i.e., the precise energy ordering) can depend on the length of the chain and on the considered impurity (compare Figs. 5 and 6). However, the correlation between symmetry and degree of delocalization holds in all cases.

D. Dependence on the interatomic distances

Real wires are not free standing but deposited on substrates or eventually created as the result of stretching a tip-surface contact in an STM experiment. In both cases, the interaction with the environment introduces strain and changes in the interatomic distances with respect to the optimal bond length. In order to investigate the effects of strain on the electronic and magnetic properties of the wires, we have performed calculations of the relative stability ΔE_m of the different total spin polarizations and of the corresponding impurity moments μ_α (α=Ni or Co) as a function of the interatomic distance d. For simplicity, all NN distances (between the impurity and the host, and between the Cu atoms) are taken to be the same ($d_{ij}=d$ for all NN ij).

In Figs. 7 and 8 results are given for Cu_4NiCu_4 and Cu_4CoCu_4 wires. First of all, one observes that the ground-state total spin is quite robust. For all considered values of d the lowest-energy spin configuration is $S_z=1$ for Ni-doped chains and $S_z=3/2$ for Co-doped chains. The excitation energy to the LS state ($S_z=0$ or 1/2) gives a measure of the

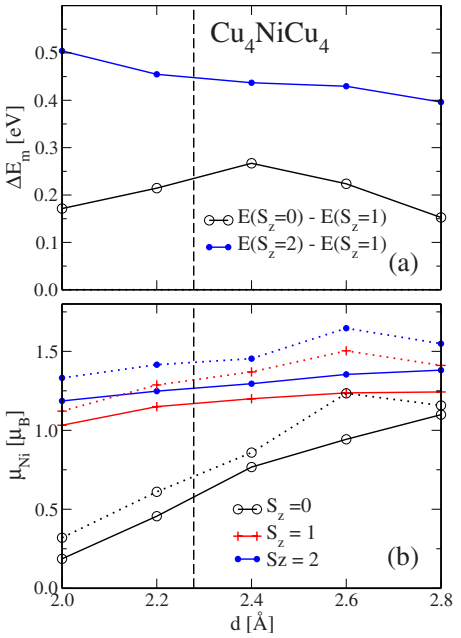

FIG. 7. (Color online) Electronic and magnetic properties of symmetric Cu_4NiCu_4 wires as a function of the nearest neighbors distance d: (a) magnetic excitation energies ΔE_m relative to the ground state having $S_z=1$, (b) local magnetic moment on the Ni atom, in the Wigner Seitz sphere (full line) and the Bader atomic cell (dotted lines). Circles refer to $S_z=0$, crosses to $S_z=1$, and dots to $S_z=2$. The lines connecting the points are a guide to the eyes. The vertical dashed line indicates the equilibrium CuNi distance of the fully relaxed chain for $S_z=1$.

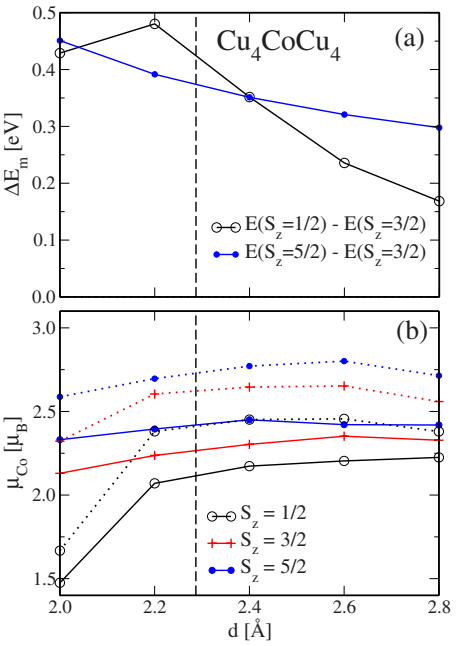

FIG. 8. (Color online) Electronic and magnetic properties of symmetric Cu_4CoCu_4 wires as a function of the nearest neighbors distance d: (a) magnetic excitation energies ΔE_m relative to the ground state having $S_z=3/2$, (b) local magnetic moment on the Co atom, in the Wigner Seitz sphere (full line) and the Bader atomic cell (dotted lines). Circles refer to $S=1/2$, crosses to $S_z=3/2$ and dots to $S_z=5/2$. The lines connecting the points are a guide to the eyes. The vertical dashed line indicates the equilibrium CuCo distance of the fully relaxed chain for $S_z=3/2$.

stability of FM versus AF-like coupling between the impurity and the conduction electrons. It can therefore be regarded as an effective exchange coupling between the impurity and Cu moments. $\Delta E_{\mathrm{LS}}=E(0,1/2)-E(1,3/2)$ shows a non- monotonous behavior as a function of d, with a maximum near the interatomic distance yielding the lowest total energy (dashed vertical line). Qualitatively, this reflects the interplay between the hybridizations and the local exchange and correlation. On the one side, for long distances and vanishing hybridizations, the differences between FM and AF coupling become immaterial and therefore ΔE_{LS} decreases. On the other side, for short d, the hybridizations start to dominate, bonding and electron delocalization are favored, which tends to stabilize the LS state. In contrast, the excitation energy to the HS state ($S_z=2$ or 5/2) increases monotonously with decreasing d, at least in the considered range. This is consistent with previous results showing that increasing the total spin beyond $S_z=1$ or 3/2 consists essentially in a single-particle spin-excitation within the Cu conduction band. In the present context the stronger hybridizations for short d imply larger single-particle gaps, which increase $\Delta E_{\mathrm{HS}}=E(2,5/2)-E(1,3/2)$.

Concerning the impurity moments μ_α, one observes nearly saturated μ_{Ni} and μ_{Co} for $S_z\geq 1$, which are essentially unaffected by reasonable changes in d [see Figs. 7(b) and 8(b)]. In most cases only a slight increase in μ_α is discerned as we approach the atomic limit. In contrast, in the LS state ($S_z=0$ or 1/2) the impurity moment is much more sensitive to variations in the interatomic hybridization, particularly for small distances where μ_α is far from saturation. The strong increase in μ_{Ni} with increasing d_{NiCu} can be understood as the result of the interplay between the exchange interaction at the impurity orbital and the hybridization of the latter with its Cu NNs. As d_{NiCu} increases, the overlap between the impurity d orbitals and the Cu s orbitals decreases. This reduces the importance of the kinetic or bonding energy (hybridization) relative to the local exchange energy, thus favoring the formation of a local Ni moment. For a large d_{NiCu}, as well as for $S_z=1$ or $S_z=2$, the Ni moment reaches saturation ($\mu_d \simeq 10-\nu_d$) and is therefore nearly independent of d_{NiCu}. Moreover, the usual stronger stability of magnetism in the case of Co explains that even in the LS state μ_{Co} reaches saturation faster than μ_{Ni} with increasing d. For Co this occurs already for values below the equilibrium distance d_{CoCu} while for Ni the local moment saturates only for $d\geq 2.8$ Å. It is only for these large distances that μ_{Ni} in the LS state becomes comparable to the impurity moment in the ground state or in the HS state. In sum, one concludes that the electronic and magnetic properties of the wires are qualitatively robust. However, depending on the type of impurity and on the considered property, the quantitative results may be modified by strain and by the resulting changes in the interatomic distances.

E. Role of the impurity position

Impurity position and wire symmetry can be manipulated in experiment and could thus provide a means of tuning the

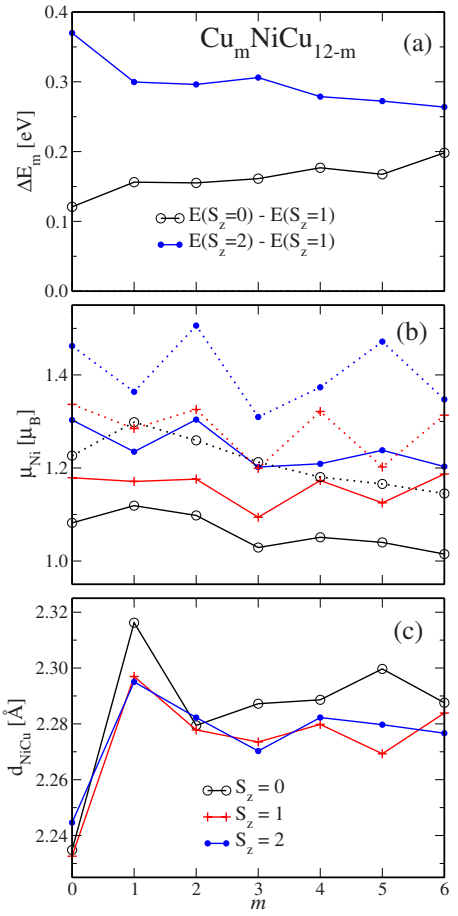

FIG. 9. (Color online) Electronic, magnetic, and structural properties of Cu_mNiCu_{12-m} wires as a function of the Ni impurity position given by m: (a) magnetic excitation energy $\Delta E_m = E(S_z) - E(S_z = 1)$ with respect to the ground state having $S_z = 1$, (b) local magnetic moment at the Ni atom within the Wigner-Seitz sphere (full lines) and the Bader atomic cell (dotted lines), and (c) equilibrium interatomic distance d_{NiCu} between the Ni impurity and its Cu nearest neighbors. Circles refer to $S_z = 0$, crosses to $S_z = 1$, and dots to $S_z = 2$. The lines connecting the points are a guide to the eyes.

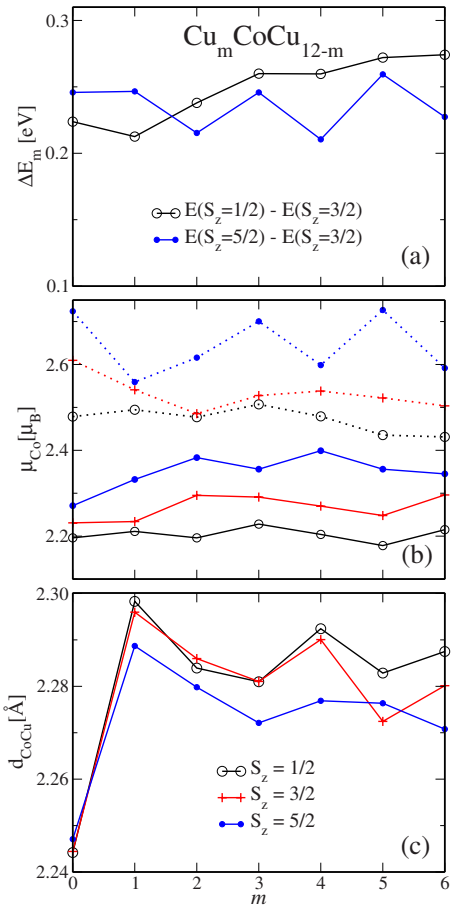

FIG. 10. (Color online) Electronic, magnetic, and structural properties of Cu_mCoCu_{12-m} wires as a function of the Co impurity position given by m: (a) magnetic excitation energy $\Delta E_m = E(S_z) - E(S_z = 3/2)$ with respect to the ground state having $S_z = 3/2$, (b) local magnetic moment at the Co atom within the Wigner-Seitz sphere (full lines) and the Bader atomic cell (dotted lines), and (c) equilibrium interatomic distance d_{CoCu} between the Co impurity and its Cu nearest neighbors. Circles refer to $S_z = 1/2$, crosses to $S_z = 3/2$, and dots to $S_z = 5/2$. The lines connecting the points are a guide to the eyes.

properties of magnetic impurities in 1D systems. It is therefore interesting to investigate the electronic, structural, and magnetic properties of doped chains as a function of the position of the impurity within the wire. To this aim we have performed calculations for chains having a fixed length and varied the number of atoms m at one side of the impurity. To be explicit we consider 12 Cu atoms and one Ni or Co impurity, so that the wires have the form Cu_mNiCu_{12-m} and Cu_mCoCu_{12-m}, Thus, $m = 0$ corresponds to the impurity at the edge of the wire, and $m = 6$ to the previously considered case of the impurity at the center of the wire.

The results are summarized in Figs. 9 and 10. First of all, one observes that the ground-state spin is the same for all impurity positions. Moreover, there are no important quantitative changes in the magnetic excitation energy ΔE_m from the ground state to the LS or HS states. However, the relative stability of the different spin solutions shows some interesting trends which deserve to be pointed out. In the case of Ni the excitation energy to the LS state ΔE_{LS} decreases slightly as the impurity is moved from the center to edge of the wire while the excitation energy to the HS state ΔE_{HS} shows the opposite trend. This reflects the environment dependence of the spin polarizability of the Cu wire at different atomic positions. The effect could be related to changes in the NiCu NN distance, which is shorter when the impurity occupies the edge position than when it is at the center of the wire [see Fig. 9(c)]. As discussed in the previous section, shorter distances imply stronger hybridization, which tends to stabilize the LS state and to destabilize the HS state. The reduction in coordination number alone, i.e., the picture that at the edge position the impurity approaches the atomic limit, does not seem a plausible explanation since under this assumption one would expect the gap between LS and HS states to be reduced (see also Fig. 7).

In the case of Co-doped wires one observes an interesting level crossing between the first and second excited spin-states as a function of the impurity position. Let us recall, that for symmetric not too short wires, the $S_z = 5/2$ configu-

ration is slightly more stable than the $S_z=1/2$ state. As we move the impurity away from the center of the wire the LS state tends to be stabilized with respect to the HS state and eventually becomes more stable when the impurity occupies the edge or near-edge position. This is in agreement with the trend observed for Ni-doped wires. Moreover, one also observes oscillations of ΔE_{HS} as a function of m, which appear to correlate with similar oscillations in the impurity moment within the Bader cell [compare Figs. 10(a) and 10(b)].

The dependence of the magnetic moment at the Ni or Co atoms on the impurity position is found to be relatively weak in absolute values, typically on the order of 5–10 %. This holds in particular for Co, which confirms the robustness and nearly saturated character of its magnetic moment. Comparing central and edge positions in the LS state of Ni, a weak tendency to an enhancement of the local moments can be discerned. This is consistent with the enhancement of μ_{Ni} as we approach the atomic limit, i.e., for increasing NN distance d, as shown in Fig. 7. Notice that the WS and Bader moments follow similar trends in general, although the environment dependence of the Bader moments is often somewhat stronger. Let us finally point out that the NN distance around the impurity depends very weakly on the impurity position, showing weak oscillations as a function of m. The strongest effect is found when the impurity lies at the edge, where a bond-length contraction of about 2% is observed. Similar reductions in the NN distances are found in low-coordinated small clusters.[22]

IV. SUMMARY AND OUTLOOK

The electronic and magnetic properties of Co and Ni impurities in finite Cu wires have been investigated in the framework of a generalized gradient approximation to density-functional theory. The problem of local moment formation in 1D systems has been analyzed in some detail from a first-principles perspective. To this aim, a number of physical properties of the low-lying spin states have been determined as a function of experimentally relevant parameters such as wire length, NN impurity-host distance and impurity position within the wire. The discussion includes the relative stability of the different total spin configurations, the local impurity moment in both Wigner-Seitz and Bader cells, the impurity-host equilibrium distance, the local electronic structure at the impurity, the induced magnetic moments in the 1D metal host, as well as their order with respect to the impurity moment.

The qualitatively most important outcome of the calculations is that the optimal total spin S_z is not minimal but one above minimal. Indeed, for a broad range of considered wires having an even number of Cu atoms we obtain that the ground-state spin configuration is $S_z=1$ for Ni-doped wires and $S_z=3/2$ for Co-doped wires. Both Co and Ni impurities preserve their magnetic degree of freedom and develop large, nearly saturated local magnetic moments in all low-lying spin configurations ($S_z \leq 5/2$).

In the ground-state spin configuration ($S_z=1$ or 3/2) the magnetic coupling between the impurity moment and the moments induced at the host atoms is ferromagneticlike, with no sign of spin fluctuations or Kondo screening. This indicates that the local exchange energy dominates over the hybridization and spin-fluctuation effects, at least within the framework of the present GGA to DFT. This behavior is found to be qualitatively very robust, as reflected by the obtained dependences on bond-length and impurity position. It should be also noted that the stability of the magnetic degree of freedom is in general weaker for Ni than for Co. Consequently, the former is more easily affected by changes in the local atomic environment.

The results for the local density of electronic states at the impurity atoms confirm that the impurity moments are largely dominated by the d-electron contributions. Moreover, a 100% minority-spin polarization of the electronic states at the Fermi energy is observed. A more detailed analysis of the corresponding d wave functions reveals a remarkable correlation between the rotational symmetry and the degree of delocalization of the impurity states, which should be detectable in STM experiments.

The present investigations deserve to be extended in a number of new directions. It would be interesting to study the magnetic interactions between two magnetic impurities in a 1D host[13] in order to quantify Ruderman-Kittel-Kasuya-Yoshida-type interactions as it has been done in the case of Cu surfaces.[5–7] Moreover, the effects of the interactions with experimentally relevant insulating and metallic substrates should be quantified. In fact, these can affect not only the details of the wire geometry but also the wire electronic structure, particularly in the case of metallic supports. More extended calculations of additional electronic properties such as spin-density profiles would also provide further possibilities of contrasting theory and experiment.

From a more fundamental perspective, the interplay between local exchange and Kondo spin fluctuations should be investigated in more detail, in order to achieve rigorous conclusions concerning the ground-state and low-lying spin configurations. The inherent difficulties in describing dynamical Kondo screening and the energy lowering associated to fluctuations of the local spin degrees of freedom with the available exchange and correlation density functionals motivate explicitly correlated studies going beyond the usual mean-field approximations. Multiband model Hamiltonians[4] with parameters derived from the present calculations, as well hybrid localized-molecular *ab initio* methods,[34] offer interesting realizable perspectives for the near future.

ACKNOWLEDGMENTS

This work has been supported by the Deutsche Forschungsgemeinschaft through the Priority Program "Nanowires and Nanotubes" and by the DAAD-CONACyT exchange program PROALMEX. Computer resources provided by Centro Nacional de Supercómputo (IPICyT), the Jülich Supercomputing Centre, and the IT Service Center of the University of Kassel are gratefully acknowledged.

[1] G. A. Prinz, Science **282**, 1660 (1998); S. A. Wolf, A. Y. Chtchelkanova, and D. M. Treger, IBM J. Res. Dev. **50**, 101 (2006).

[2] J. Bansmann, S. H. Baker, C. Binns, J. A. Blackman, J.-P. Bucher, J. Dorantes-Dávila, V. Dupuis, L. Favre, D. Kechrakos, A. Kleibert, K.-H. Meiwes-Broer, G. M. Pastor, A. Perez, O. Toulemonde, K. N. Trohidou, J. Tuaillon, and Y. Xie, Surf. Sci. Rep. **56**, 189 (2005).

[3] P. Gambardella, A. Dallmeyer, K. Maiti, M. C. Malagoli, W. Eberhardt, K. Kern, and C. Carbone, Nature (London) **416**, 301 (2002); P. Gambardella, A. Dallmeyer, K. Maiti, M. C. Malagoli, S. Rusponi, P. Ohresser, W. Eberhardt, C. Carbone, and K. Kern, Phys. Rev. Lett. **93**, 077203 (2004).

[4] J. Dorantes-Dávila and G. M. Pastor, Phys. Rev. Lett. **81**, 208 (1998); R. Félix-Medina, J. Dorantes-Dávila, and G. M. Pastor, New J. Phys. **4**, 100 (2002).

[5] F. Silly, M. Pivetta, M. Ternes, F. Patthey, J. P. Pelz, and W.-D. Schneider, Phys. Rev. Lett. **92**, 016101 (2004); M. Ternes, C. Weber, M. Pivetta, F. Patthey, J. P. Pelz, T. Giamarchi, F. Mila, and W.-D. Schneider, *ibid.* **93**, 146805 (2004).

[6] N. Knorr, H. Brune, M. Epple, A. Hirstein, M. A. Schneider, and K. Kern, Phys. Rev. B **65**, 115420 (2002); V. S. Stepanyuk, A. N. Baranov, D. V. Tsivlin, W. Hergert, P. Bruno, N. Knorr, M. A. Schneider, and K. Kern, *ibid.* **68**, 205410 (2003).

[7] V. S. Stepanyuk, L. Niebergall, R. C. Longo, W. Hergert, and P. Bruno, Phys. Rev. B **70**, 075414 (2004).

[8] O. Fruchart, J.-C. Toussaint, P.-O. Jubert, W. Wernsdorfer, R. Hertel, J. Kirschner, and D. Mailly, Phys. Rev. B **70**, 172409 (2004); W. Wernsdorfer, N. E. Chakov, and G. Christou, *ibid.* **70**, 132413 (2004); M. Jamet, W. Wernsdorfer, C. Thirion, V. Dupuis, P. Mélinon, A. Pérez, and D. Mailly, *ibid.* **69**, 024401 (2004); C. Portemont, R. Morel, W. Wernsdorfer, D. Mailly, A. Brenac, and L. Notin, *ibid.* **78**, 144415 (2008).

[9] R. Félix-Medina, J. Dorantes-Dávila, and G. M. Pastor, Phys. Rev. B **67**, 094430 (2003).

[10] S. Lounis, P. H. Dederichs, and S. Blügel, Phys. Rev. Lett. **101**, 107204 (2008).

[11] J. Lagoute, X. Liu, and S. Fölsch, Phys. Rev. B **74**, 125410 (2006).

[12] J. Lagoute, C. Nacci, and S. Fölsch, Phys. Rev. Lett. **98**, 146804 (2007).

[13] C. Liu, T. Uchihashi, and T. Nakayama, Phys. Rev. Lett. **101**, 146104 (2008).

[14] X.-D. Ma, D. I. Bazhanov, O. Fruchart, F. Yildiz, T. Yokoyama, M. Przybylski, V. S. Stepanyuk, W. Hergert, and J. Kirschner, Phys. Rev. Lett. **102**, 205503 (2009).

[15] H. Oka, P. A. Ignatiev, S. Wedekind, G. Rodary, L. Niebergall, V. S. Stepanyuk, D. Sander, and J. Kirschner, Science **327**, 843 (2010).

[16] *Valence Fluctuations in Solids*, edited by L. M. Falicov, W. Hanke, and M. B. Maple (North-Holland, Amsterdam, 1981); *Valence Instabilities*, edited by P. Wachter and H. Boppart (North-Holland, Amsterdam, 1982); P. Fulde, *Electron Correlations in Molecules and Solids* (Springer, Berlin, 1993).

[17] J. Kondo, Prog. Theor. Phys. **32**, 37 (1964).

[18] A. C. Hewson, *The Kondo Problem to Heavy Fermions* (Cambridge University, Cambridge, 1997).

[19] P. W. Anderson, Phys. Rev. **124**, 41 (1961).

[20] W. B. Thimm, J. Kroha, and J. von Delft, Phys. Rev. Lett. **82**, 2143 (1999); P. Schlottmann, Philos. Mag. Lett. **81**, 575 (2001); P. S. Cornaglia and C. A. Balseiro, Phys. Rev. B **66**, 115303 (2002).

[21] G. M. Pastor, Ann. Phys. **14**, 547 (2005); J. L. Ricardo-Chávez and G. M. Pastor, Comput. Mater. Sci. **35**, 311 (2006).

[22] J. L. Ricardo-Chávez and G. M. Pastor (unpublished).

[23] N. Néel, J. Kröger, R. Berndt, T. O. Wehling, A. I. Lichtenstein, and M. I. Katsnelson, Phys. Rev. Lett. **101**, 266803 (2008).

[24] P. Wahl, P. Simon, L. Diekhöner, V. S. Stepanyuk, P. Bruno, M. A. Schneider, and K. Kern, Phys. Rev. Lett. **98**, 056601 (2007).

[25] A. F. Otte, M. Ternes, K. von Bergmann, S. Loth, H. Brune, C. P. Lutz, C. F. Hirjibehedin, and A. J. Heinrich, Nat. Phys. **4**, 847 (2008).

[26] P. Hohenberg and W. Kohn, Phys. Rev. **136**, B864 (1964); W. Kohn and L. J. Sham, *ibid.* **140**, A1133 (1965).

[27] G. Kresse and J. Furthmüller, Phys. Rev. B **54**, 11169 (1996); G. Kresse and D. Joubert, *ibid.* **59**, 1758 (1999).

[28] Y. Wang and J. P. Perdew, Phys. Rev. B **44**, 13298 (1991); J. P. Perdew and Y. Wang, *ibid.* **45**, 13244 (1992); J. P. Perdew, J. A. Chevary, S. H. Vosko, K. A. Jackson, M. R. Pederson, D. J. Singh, and C. Fiolhais, *ibid.* **46**, 6671 (1992).

[29] P. E. Blöchl, Phys. Rev. B **50**, 17953 (1994).

[30] G. Kresse and J. Furthmüller, VASP the Guide, http://cms.mpi.univie.ac.at/vasp/

[31] N. D. Mermin, Phys. Rev. **137**, A1441 (1965); M. Methfessel and A. T. Paxton, Phys. Rev. B **40**, 3616 (1989).

[32] R. Bader, *Atoms in Molecules: A Quantum Theory* (Oxford University Press, New York, 1990).

[33] G. Henkelman, A. Arnaldsson, and H. Jónsson, Comput. Mater. Sci. **36**, 354 (2006); E. Sanville, S. Kenny, R. Smith, and G. Henkelman, J. Comput. Chem. **28**, 899 (2007).

[34] N. Suaud, G. M. Pastor, S. Evangelisti, and D. Maynau, Chem. Phys. Lett. **378**, 503 (2003).